SSD-TR-90-51

12

AEROSPACE REPORT NO.
TR-0089(4930-06)-1

AD-A231 366

Transverse Flow Gas Lens

Prepared by

H. MIRELS, D. J. SPENCER, and R. HOFLAND
Aerophysics Laboratory
Laboratory Operations

29 November 1990

Prepared for

SPACE SYSTEMS DIVISION
AIR FORCE SYSTEMS COMMAND
Los Angeles Air Force Base
P. O. Box 92960
Los Angeles, CA 90009-2960

Development Group

THE AEROSPACE CORPORATION
El Segundo, California

APPROVED FOR PUBLIC RELEASE;
DISTRIBUTION UNLIMITED

This report was submitted by The Aerospace Corporation, El Segundo, CA 90245-4691, under Contract No. F04701-88-C-0089 with the Space Systems Division, P.O. Box 92960, Los Angeles, CA 90009-2960. It was reviewed and approved for The Aerospace Corporation by W. P. Thompson, Director, Aerophysics Laboratory. Captain R. Riviere was the project officer for the Mission-Oriented Investigation and Experimentation (MOIE) Program.

This report has been reviewed by the Public Affairs Office (PAS) and is releasable to the National Technical Information Service (NTIS). At NTIS, it will be available to the general public, including foreign nationals.

This technical report has been reviewed and is approved for publication. Publication of this report does not constitute Air Force approval of the report's findings or conclusions. It is published only for the exchange and stimulation of ideas.

RAFAEL A. RIVIERE, Capt, USAF
MOIE Project Officer
SSD/CNL

JONATHAN M. EMMES, Maj, USAF
MOIE Program Manager
AFSTC/WCO OL-AB

UNCLASSIFIED

SECURITY CLASSIFICATION OF THIS PAGE

REPORT DOCUMENTATION PAGE

1a. REPORT SECURITY CLASSIFICATION Unclassified	1b. RESTRICTIVE MARKINGS
2a. SECURITY CLASSIFICATION AUTHORITY	3. DISTRIBUTION/AVAILABILITY OF REPORT Approved for public release; distribution unlimited.
2b. DECLASSIFICATION/DOWNGRADING SCHEDULE	
4. PERFORMING ORGANIZATION REPORT NUMBER(S) TR-0089(4930-06)-1	5. MONITORING ORGANIZATION REPORT NUMBER(S) SSD-TR-90-51
6a. NAME OF PERFORMING ORGANIZATION The Aerospace Corporation Laboratory Operations 6b. OFFICE SYMBOL (If applicable)	7a. NAME OF MONITORING ORGANIZATION Space Systems Division
6c. ADDRESS (City, State, and ZIP Code) El Segundo, CA 90245-4691	7b. ADDRESS (City, State, and ZIP Code) Los Angeles Air Force Base Los Angeles, CA 90009-2960
8a. NAME OF FUNDING/SPONSORING ORGANIZATION 8b. OFFICE SYMBOL (If applicable)	9. PROCUREMENT INSTRUMENT IDENTIFICATION NUMBER F04701-88-C-0089
8c. ADDRESS (City, State, and ZIP Code)	10. SOURCE OF FUNDING NUMBERS PROGRAM ELEMENT NO. / PROJECT NO. / TASK NO. / WORK UNIT ACCESSION NO.

11. TITLE (Include Security Classification)

Transverse Flow Gas Lens

12. PERSONAL AUTHOR(S)

Mirels, Hal; Spencer, Donald J.; and Hofland, Robert

13a. TYPE OF REPORT	13b. TIME COVERED	14. DATE OF REPORT (Year, Month, Day)	15. PAGE COUNT
	FROM ______ TO ______	1990 November 29	27

16. SUPPLEMENTARY NOTATION

* Optical lenses,

17. COSATI CODES			18. SUBJECT TERMS (Continue on reverse if necessary and identify by block number)
FIELD	GROUP	SUB-GROUP	Lasers, Optical Beam Control, Free electron lasers, Optics, * [illegible]

19. ABSTRACT (Continue on reverse if necessary and identify by block number)

The concept of a transverse flow gas lens is described. In this device, gas flows between two parallel plates which are heated or cooled so as to generate a parabolic variation of index of refraction in the region between the plates. A laser beam, propagating normal to the gas flow, can then be diverged, converged, or focused. A single module acts like a cylindrical lens. The use of two or three modules, arranged in an orthogonal manner, provides a spherical lens. Equations and tables are provided for the design of one, two, and three module configurations. The advantages of the transverse flow gas lens (relative to a device with flow along the optic axis) are (a) thermal blooming is minimized (due to short residence time of fluid in laser beam), (b) the index of refraction profile is the same throughout each module, leading to good beam quality, and (c) the system is readily scaleable. However, a longer distance along the optical axis may be needed by the transverse flow lens. 25

20. DISTRIBUTION/AVAILABILITY OF ABSTRACT ☒ UNCLASSIFIED/UNLIMITED ☐ SAME AS RPT ☐ DTIC USERS	21. ABSTRACT SECURITY CLASSIFICATION Unclassified
22a. NAME OF RESPONSIBLE INDIVIDUAL	22b. TELEPHONE (Include Area Code) / 22c. OFFICE SYMBOL

DD FORM 1473, 84 MAR — 83 APR edition may be used until exhausted. All other editions are obsolete

SECURITY CLASSIFICATION OF THIS PAGE

UNCLASSIFIED

CONTENTS

FIGURES

TABLES

I. INTRODUCTION

It is known that gases transported within a tube can act to diverge, collimate, or focus a beam of light directed along the axis of the tube. It is also known that high-intensity laser light can damage solid lenses. Thus, a lens constructed using a gas flow with low light absorption is of interest because of its ability to accommodate high light intensities that would otherwise damage solid lenses.

A pipe flow gas lens concept has been proposed by Marcuse, et al.[1] In this concept, a laser beam is propagated through a cooled rotating pipe which confines a relatively warm flowing gas (Fig. 1a). As shown in Fig. 1b, the radial temperature variation of the gas flowing in the pipe produces a radial refractive index variation which corresponds to a negative optical lens. The use of a warm pipe and a relatively cool gas, as discussed in Ref. 1, produces a positive optical lens. A more recent discussion of the performance of the pipe flow gas lens, as well as its application as a defocusing optical element in free electron lasers, has been given by Christiansen.[2]

There are several shortcomings associated with the pipe flow gas lens concept. First, the radial variation of the index of refraction is not parabolic in the pipe inlet boundary-layer region. This nonparabolic index variation may produce aberrations that degrade beam quality. Second, at high optical intensities, these devices are susceptible to distortions caused by heating of the gas and thermal blooming because of the long dwell time of the gas in the laser beam path. The amount of distortion increases as the beam travels along the optic axis. Third, these devices are not scaleable because optical effectiveness is reduced in the downstream flow region due to gas-wall temperature equilibration, as indicated in Fig. 1b.

The above limitations can be circumvented by the use of a gas flow which is transverse rather than parallel to the optical axis. This

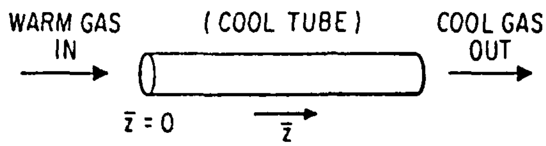

(a) CONFIGURATION OF REF. 1

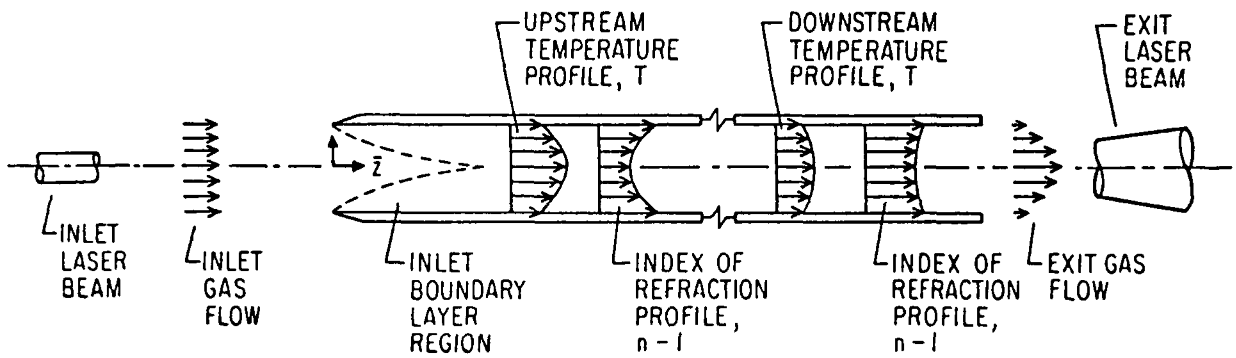

(b) TEMPERATURE AND INDEX OF REFRACTION PROFILES

Fig. 1. A Schematic Diagram of a Pipe Flow Gas Lens (Ref. 1). A negative (divergent) lens is illustrated.

concept, termed a transverse flow gas lens, is illustrated in Figs. 2 to 5 for the case of a negative optical lens (i.e., cooled wall) which is of interest as a beam-diverging element in a free electron laser.[2] A high quality gas lens module, for control of a laser beam, can be established by generating a fully developed thermal boundary-layer gas flow between two cooled parallel plates as indicated in Fig. 2a. When a laser beam is

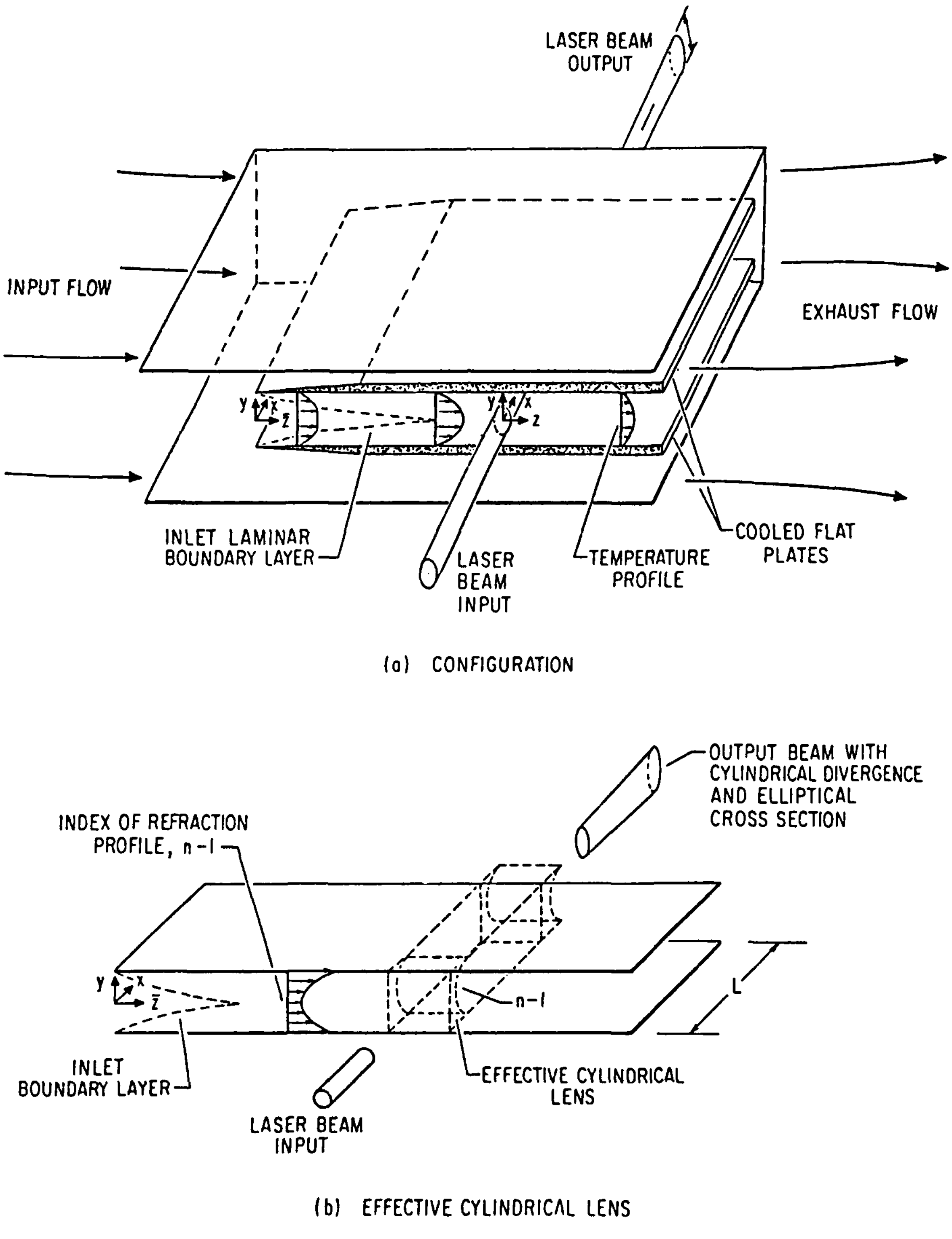

Fig. 2. A Schematic Diagram of One Module of a Transverse Flow Gas Lens. For the case of a collimated input beam with circular cross section, this configuration provides an exit beam with cylindrical divergence and elliptical cross section.

propagated transverse to the flow direction in the fully developed thermal boundary layer region, a cylindrical divergence of the beam is produced as shown in Fig. 2b. Two such modules, mounted in line with the laser beam path and with gas flow directions orthogonal to one another, provide an exit beam with a spherical wave front and an elliptical cross section as shown in Fig. 3. As shown in Fig. 4, three modules can be mounted in line to generate an exit beam with a spherical wavefront and a circular cross section, functioning as a single spherical diverging lens. The array depicted in Fig. 4 may be considered a three module system in which the central module, operating on the z beam component, is sandwiched between and orthogonal to the two bookend modules that operate on the y beam component. A schematic representation of optical ray paths through a three module system is shown in Fig. 5.

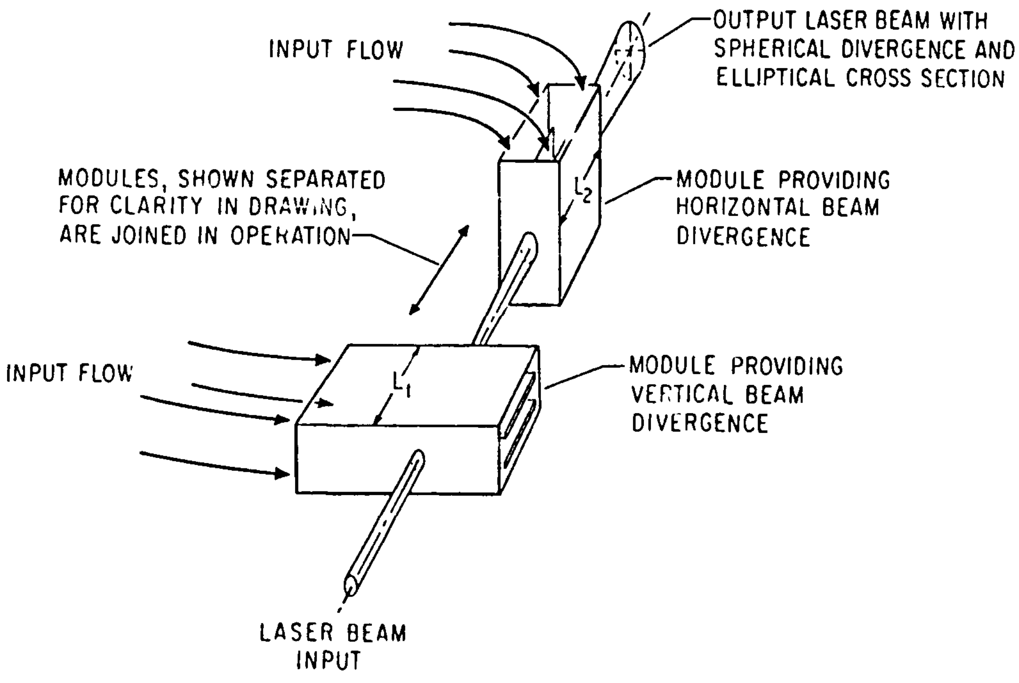

Fig. 3. A Schematic Diagram of Two Orthogonal Modules of a Transverse Flow Gas Lens. For the case of a collimated input beam with circular cross section, these modules provide an exit beam with spherical divergence and elliptical cross section.

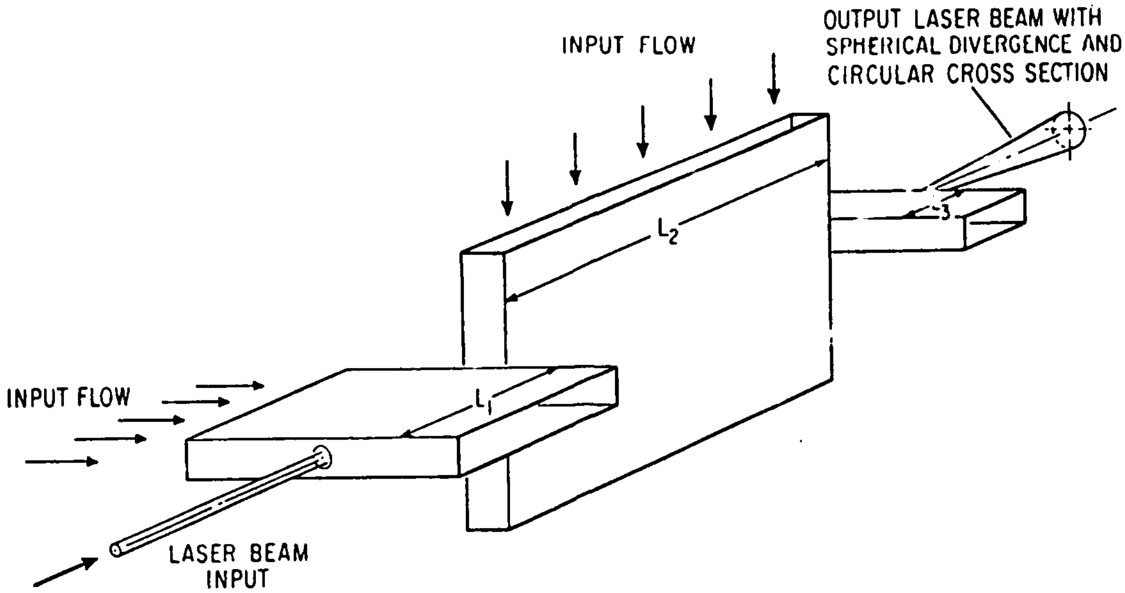

Fig. 4. A Schematic Diagram of a Three Module Transverse Flow Gas Lens. For the case of a collimated input beam with circular cross section, this configuration provides an exit beam with spherical divergence and circular cross section.

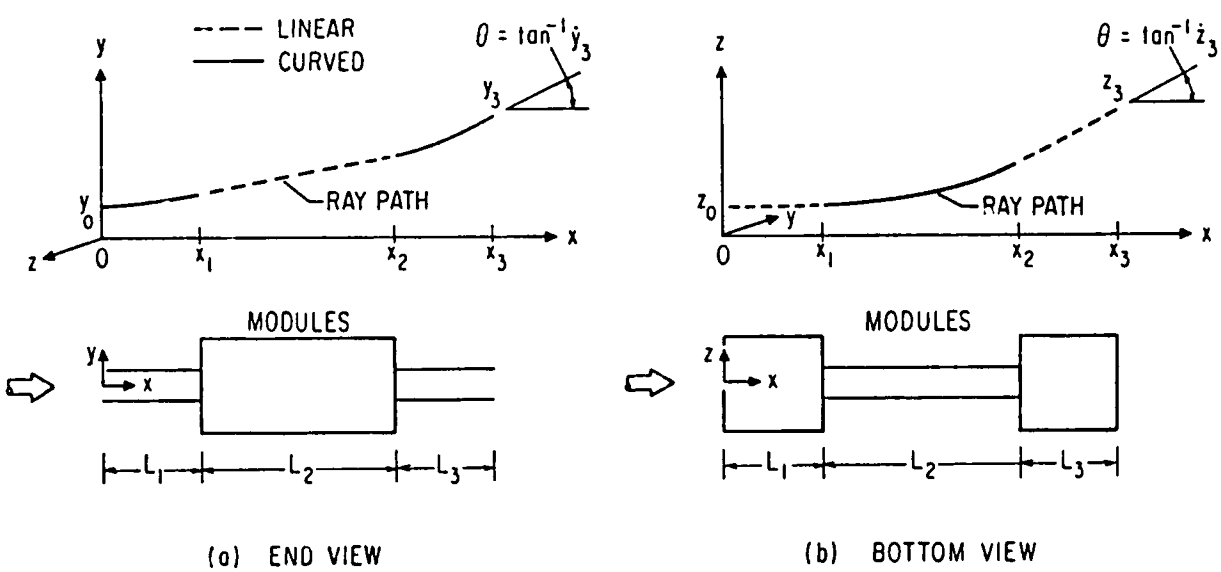

Fig. 5. Ray Paths Through Orthogonal Components of a Three Unit Transverse Flow Gas Lens

In this report we discuss the performance of a transverse flow gas lens. Thermal boundary layer development, index of refraction profiles, and optical ray paths are discussed. Designs of one, two, and three module systems are then noted.

II. THEORY

A. THERMAL BOUNDARY LAYER

The thermal boundary layer development is assumed to consist of an inlet region and a fully developed flow region as illustrated in Fig. 6. The thermal boundary layer growth in the inlet region is estimated using the conventional semi-infinite laminar flat plate expression. Thus, the thermal boundary layer growth along the flow direction is described approximately, by[3]

$$\delta_{th} = 5(\mu\bar{z}/\rho v)^{1/2}\ Pr^{-1/3} \tag{1}$$

where $\bar{z}$ denotes streamwise distance measured from the leading edge of the cooled plate, δ_{th} is the thermal boundary layer thickness, v is the gas velocity in the streamwise direction, μ, k, ρ, and C_p are the gas viscosity, thermal conductivity, density, and heat capacity, and $Pr = \mu\ C_p/k$ is the gas Prandtl number. The latter gas properties are based on the average boundary layer temperature. The thermal boundary layer development is shown schematically by the labeled dashed curve in Fig. 6. Typical values of flow parameters are included in Fig. 6 for the case of an argon gas and walls cooled by liquid oxygen.

Boundary layer closure occurs when $2\delta_{th} = D$, where D is the plate separation distance. The corresponding streamwise location is denoted $\bar{z}_c$ and is found from

$$\bar{z}_c/v = (D^2/100)\ (\rho/\mu)\ (Pr)^{2/3} \tag{2}$$

Note that for fixed D and gas properties, z_c varies linearly with v. It is necessary that the flow remain laminar upstream of the closure region in order to assure an optical medium with good beam quality. A criterion for laminar flow in this region is $Re_c \equiv \rho v z_c/\mu \equiv [(\rho v D)/10\mu)]^2\ \ Pr^{2/3} \lesssim 10^5$, where Re_c is the Reynolds number based on inlet length z_c.

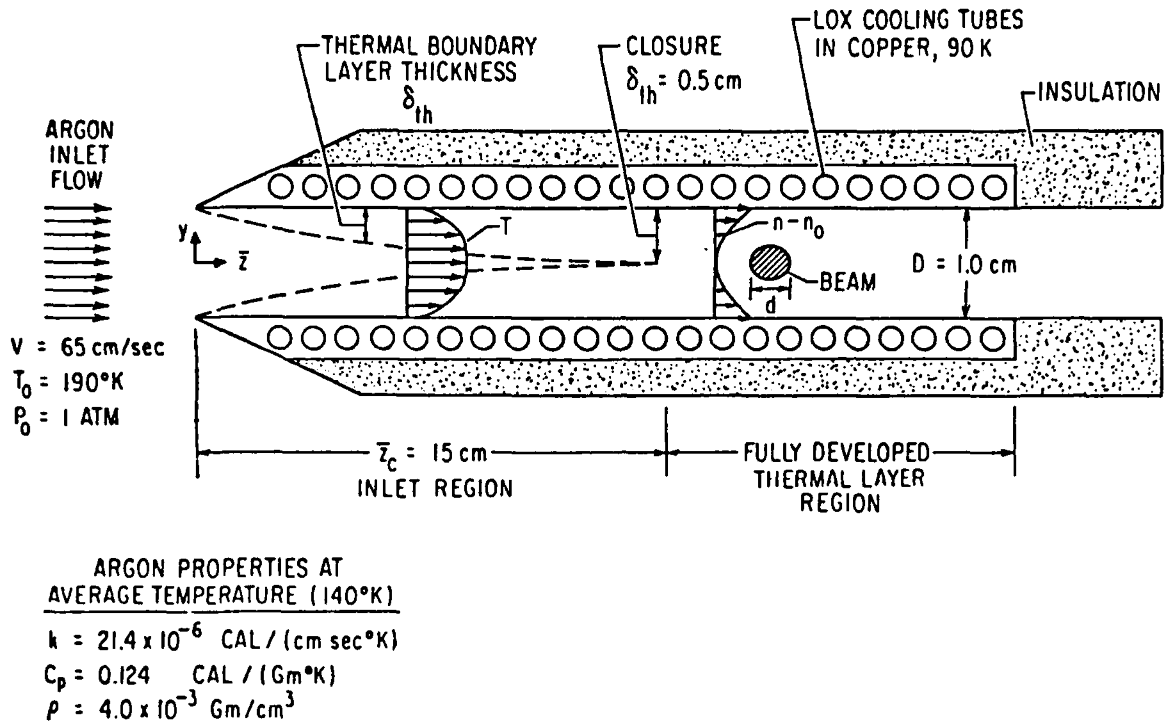

Fig. 6. A Schematic Diagram Showing Thermal Boundary Layer Growth Between Two Cooled Plates

Downstream of the boundary layer closure region the fluid temperature profile may be approximated by

$$\frac{T_0 - T}{T_0 - T_w} = (2y/D)^2 \tag{3}$$

where T_0 and T_w denote local centerline and local wall temperatures, respectively, and y denotes lateral distance from the centerline. The variation of index of refraction with gas properties is given by an expression in Table 1. Assuming an ideal gas and a negligible pressure varation in the y direction, the correponding index of refraction variation is

$$\frac{n - n_0}{n_w - n_0} = (2y/D)^2 (T_w/T) \tag{4}$$

Table 1. Index of Refraction for Various Gases at Wavelength $\lambda = 5893$ Å

Note, $n - 1 = \beta \times P(atm)\ [273/T°(K)]$

GAS	AIR	N_2	CO_2	Ar	He
$\beta \times 10^4$	2.9	3.0	4.5	2.8	0.36

An optical beam, of diameter $d \ll D$, which propagates in the x direction, encounters an essentially parabolic index variation given by

$$\frac{n - n_0}{n_w - n_0} = \left(\frac{2y}{D}\right)^2 \frac{T_w}{T_0} \left[1 + O\left(1 - \frac{T_w}{T_0}\right)\left(\frac{d}{D}\right)^2\right] \tag{5}$$

The index variation in Eq. (5) is equivalent to a diverging cylindrical lens when $T_w < T_0$ (i.e., $n_w > n_0$) and is equivalent to a converging cylindrical lens when $T_w > T_0$ (i.e., $n_w < n_0$). The optical performance of these lenses is described in the next section.

B. OPTICAL PERFORMANCE

We consider multiple module configurations, wherein the laser beam propagates in the x direction. The beam entrance and exit station for the i^{th} module is denoted x_{i-1} and x_i, respectively, and the length of each module, in the beam direction, is $L_i = x_i - x_{i-1}$ (Fig. 5).

We first consider modules where the flow is in the $\bar{z}$ direction and denote downstream distance, measured from the beam centerline, by z (Fig. 2a). We assume a parabolic index variation in the y direction and a negligible index variation in the z direction. These conditions apply for

modules 1 and 3 in Fig. 5. The variation of ray ordinates y and z with distance along the beam is, in general[4]

$$\frac{\partial^2 y}{\partial x^2} = \frac{\partial n}{\partial y} \tag{6a}$$

$$\frac{\partial^2 z}{\partial x^2} = \frac{\partial n}{\partial z} \tag{6b}$$

For the parabolic index variation in the y direction [given by Eq. (5)] and no index variation in the z direction, Eq. (6) becomes

$$\frac{\partial^2 y}{\partial x^2} = A_i^2 y \tag{7a}$$

$$\frac{\partial z}{\partial x} = 0 \tag{7b}$$

where

$$A_i^2 = \left[8T_w/T_0(n_w - n_0)/D^2\right]_i \tag{7c}$$

Note that A_i is real for $n_w > n_0$, which is the case of primary interest, and A_i is imaginary for $n_w < n_0$. Let y_{i-1}, z_{i-1} and y_i, z_i denote beam ordinates at the entrance and exit of the i^{th} model, respectively. Integration of Eq. (7a) for A_i real yields

$$y_i = y_{i-1} \cosh A_i L_i + \left[(\dot{y}_{i-1})/A_i\right] \sinh A_i L_i \tag{8a}$$

$$\dot{y}_i = A_i y_{i-1} \sinh A_i L_i + \dot{y}_{i-1} \cosh A_i L_i \tag{8b}$$

When A_i is imaginary, the hyperbolic functions in Eqs. (8a) and (8b) are replaced by the corresponding trigonometric functions of $|A_i|L_i$. Integration of Eq. (7b) yields

$$z_i = z_{i-1} + \dot{z}_{i-1}L_i \tag{8c}$$

$$\dot{z}_i = \dot{z}_{i-1} \tag{8d}$$

which represents a linear variation.

The ordinates y and z are reversed in Eqs. (7) and (8) for modules with a parabolic index variation in the z direction and no index variation in the y direction (e.g., module 2 in Fig. 5).

The above expressions are used in the following subsections to obtain the performance of gas lenses with one, two, or three modules.

(1) One module configuration: A single module with flow in the z direction, beam propagation in the x direction, and a parabolic index variation in the y direction is illustrated in Figs. 2 and 7. For the case of a collimated input beam, inlet and exit ordinates are related by $z_1 = z_0$, $\dot{z}_1 = \dot{z}_0 = 0$ and

$$y_1/y_o = \cosh\,(L_1A_1) \tag{9a}$$

$$\dot{y}_1/(A_1y_o) = \sinh\,(L_1A_1) \tag{9b}$$

The output beam has a cylindrical wavefront of radius R given by

$$\frac{1 + O(y_1/R)^2}{R} = \frac{\dot{y}_1}{y_1} = A_1\,\tanh\,(A_1L_1) \tag{9c}$$

where terms of order $(y_1/R)^2$ have been neglected. Thus the module functions like a cylindrical lens. An input beam with a circular cross

section will have an elliptical cross section, with a ratio of major to minor axis equal to cosh L_1A_1, at the exit of the module. In the limit $A_1L_1 \to 0$, Eqs. (9) become $y_1 = y_0$ and

$$\frac{\dot{y}_1}{A_1 y_0} = \frac{1}{A_1 R} = A_1 L_1 \left[1 + 0 \, (A_1 L_1)^2\right] \qquad (10)$$

which is a "thin lens" approximation for module performance.

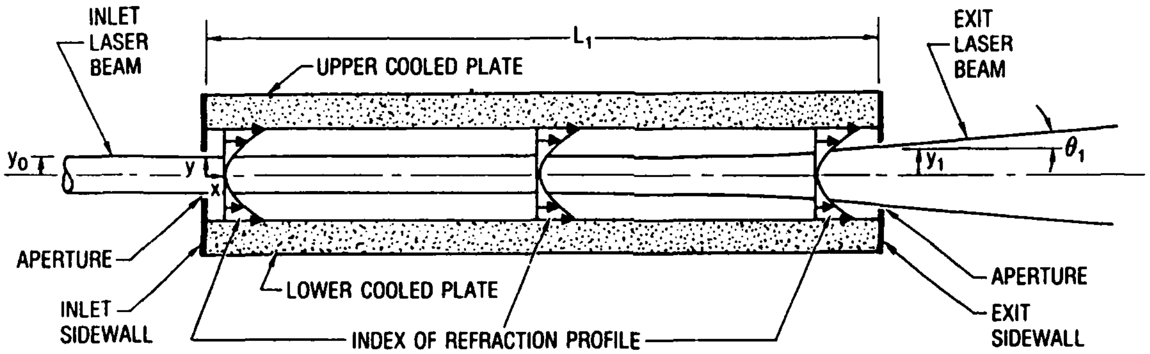

Fig. 7. A Schematic Diagram Showing Laser Beam Path Within First Module

Equations (9) have been evaluated for $0.0 \leq \dot{y}_1/A_1y_0 \leq 3.0$. The corresponding results for y_1/y_0, A_1L_1, and $1/A_1R$ are given in Table 2. These results also apply for the case of a pipe flow configuration (Fig. 1) if it is assumed that A is constant along the optical axis. Table 2 can then be used to compare the length of a pipe flow configuration with the length of an equivalent multiple module transverse flow lens designed to provide a spherically divergent output beam.

Table 2. A Table of Values Which Allow Design of a Single Module Transverse Flow Gas Lens With a Cylindrical Output Beam [see Eqs. (9)]. A collimated input beam is assumed. These results also apply for a pipe flow configuration (Fig. 1) if it is assumed that A_1 is constant along the optical axis.

$\frac{\dot{y}_1}{A_1 y_o}$	$\frac{y_1}{y_0}$	A_1L_1	$\frac{1}{A_1R}$
0.000	1.000	0.000	0.000
0.100	1.005	0.100	0.100
0.200	1.020	0.199	0.196
0.400	1.077	0.390	0.371
0.600	1.166	0.569	0.514
0.800	1.281	0.733	0.625
1.000	1.414	0.881	0.707
2.000	2.236	1.444	0.894
3.000	3.162	1.818	0.949

(2) Two module configuration: For the case of two modules with a collimated inlet beam, as indicated in Fig. 3, inlet and exit beam properties are related by

$$y_2/y_0 = \cosh A_1L_1 + A_2L_2(A_1/A_2) \sinh A_1L_1 \tag{11a}$$

$$\dot{y}_2/(A_2y_0) = (A_1/A_2) \sinh A_1L_1 \tag{11b}$$

$$z_2/z_0 = \cosh A_2L_2 \tag{11c}$$

$$\dot{z}_2/(A_2z_0) = \sinh A_2L_2 \tag{11d}$$

The exit beam will have a spherical wave front of radius R if

$$\frac{1}{R} = \frac{\dot{y}_2}{y_2} = \frac{\dot{z}_2}{z_2} \tag{12}$$

where terms of order $(y_2/R)^2$ and $(z_2/R)^2$ are neglected. If the inlet beam has a circular cross section, the exit beam will have an elliptical cross section with the ratio of major to minor axis equal to y_2/z_2. If A_1, A_2, and R are specified, Eq. (12) provides two equations for L_1 and L_2. Other properties are found from Eq. (11). For the case $A_1 = A_2 \equiv A$, it is found that

$$AL_2 = \coth^{-1}(AR) \tag{13a}$$

$$AL_1 = \coth^{-1}(AR - AL_2) \tag{13b}$$

Numerical results for this case are given in Table 3. These results were obtained by specifying $\dot{z}_2/(Az_2)$ and obtaining AL_2 from Eq. (11d). Other variables were then obtained from Eqs. (11) to (13). Eq. (13b) requires $A(R-L_2) \geq 1$ which results in the requirements $AR \geq 1.6837$, $AL_2 \leq 0.6837$, and $AL_1 \leq 5.5520$. It follows that $\dot{z}_2/(Az_2) \leq 0.7383$, $z_2/z_0 \leq 1.2430$, $\dot{y}_2/(Ay_2) \leq 128.87$ and $y_2/y_0 \leq 216.98$. These limitations do not affect the ability to design a two module gas lens since the quantity A is a design variable. The larger the value of A, the smaller the values of L_1 and L_2 required to achieve a given divergence, and the more nearly each module acts like a thin (rather than a thick) lens.

Tables 2 and 3 permit a comparison of the lengths required to achieve a given spherical divergence in a pipe flow lens (Table 2) and in a two module transverse flow lens (Table 3). For a given value of A, the latter requires approximately twice the length of the former. This is due to the fact that the pipe flow lens provides a spherical divergence at each flow station whereas the transverse flow gas lens requires a sequence of two cylindrical expansions to achieve a spherical output. A more accurate length comparison requires consideration of achievable values of A in each device and consideration of the variation of A along the optical axis in the pipe flow device.

Table 3. A Table of Values Which Allow Design of a Two Module Transverse Flow Gas Lens with Spherical Wavefront and Elliptical Cross Section Output. See Eqs. (11) to (13). Note $A_1 = A_2 = A$. A collimated input beam is assumed.

$\frac{\dot{z}_2}{Az_0}$	$\frac{z_2}{z_0}$	$\frac{\dot{y}_2}{Ay_0}$	$\frac{y_2}{y_0}$	AL_1	AL_2	$A(L_1+L_2)$	$\frac{1}{AR}$	$\frac{y_2}{z_2} - 1$
0.000	1.000	0.000	1.000	0.000	0.000	0.000	0.000	0.000
0.100	1.005	0.101	1.015	0.101	0.100	0.201	0.100	0.010
0.200	1.020	0.208	1.063	0.207	0.199	0.406	0.196	0.042
0.300	1.044	0.331	1.151	0.325	0.296	0.621	0.287	0.103
0.400	1.077	0.482	1.298	0.465	0.390	0.855	0.371	0.205
0.500	1.118	0.693	1.551	0.647	0.481	1.129	0.447	0.387
0.600	1.166	1.060	2.060	0.923	0.569	1.492	0.514	0.767
0.700	1.221	2.291	3.995	1.567	0.653	2.219	0.573	2.273
0.710	1.226	2.697	4.659	1.718	0.661	2.379	0.579	2.799
0.720	1.232	3.396	5.811	1.937	0.669	2.606	0.584	3.716
0.730	1.238	5.111	8.668	2.334	0.677	3.011	0.590	6.001
0.738	1.243	30.381	51.164	4.107	0.684	4.791	0.594	40.167

(3) Three module configuration: In the case of three modules with a collimated inlet beam, as in Fig. 4, inlet and exit beam properties are related by

$$y_3/y_0 = [\cosh A_1 L_1 + (A_2L_2)(A_1/A_2) \sinh A_1L_1] \cosh A_3L_3 + (A_1/A_3) \sinh A_1L_1 \sinh A_3L_3 \tag{14a}$$

$$\dot{y}_3/(A_3y_0) = [\cosh A_1L_1 + L_2A_2(A_1/A_2) \sinh A_1L_1] \sinh A_3L_3 + (A_1/A_3) \sinh A_1L_1 \cosh A_3L_3 \tag{14b}$$

$$z_3/z_0 = \cosh A_2L_2 + A_3L_3 (A_2/A_3) \sinh A_2L_2 \tag{14c}$$

$$\dot{z}_3/(A_3z_0) = (A_2/A_3) \sinh A_2L_2 \tag{14d}$$

The exit beam will have a spherical wave front of radius R if

$$\frac{1}{R} = \frac{\dot{y}_3}{y_3} = \frac{\dot{z}_3}{z_3} \tag{15a}$$

If the input beam is circular, the exit beam will have a circular cross section provided

$$\frac{\dot{y}_3}{y_o} = \frac{\dot{z}_3}{z_o} \tag{15b}$$

When R, A_1, A_2, and A_3 are specified, Eqs. (15) provide three equations for L_1, L_2, and L_3. The solution of these equations is simplified if the practical assumption $A_1 = A_1 = A_3 \equiv A$ is made. Numerical results for this case are given in Table 4. These results were obtained by specifying $\dot{y}_3/(Ay_0) = \dot{z}_3/(Az_0) \equiv \dot{r}_3/(Ar_0)$, obtaining AL_2 from Eq. (14d), and then obtaining the remaining variables from Eqs. (14) and (15). There does not appear to be a mathematical limitation on allowed values for $\dot{r}_3/(Ay_0)$. For small exit values of $\dot{y}/(Ay_0)$ and $\dot{z}/(Az_0)$, the two and three module transverse flow gas lens configurations give similar performance. In these cases, the two module configuration is simpler and is preferable. With an increase in exit divergence, the overall length of the three module system is less than that of the two module system for a given value of A. Moreover, the three module system provides an exit beam with a circular cross section.

Comparison of Tables 3 and 4, for small exit divergence angles, indicates that AL_1 and AL_2 in the two module configuration equal, respectively, $AL_1 + AL_3$ and AL_2 in the three module configuration. Hence, the first module in the former is split into two halves in the latter. The net length of the two and three module device is the same. With increases in exit divergence angles, the net length of the three module device tends to become smaller than that of the two module device as previously noted.

Table 4. A Table of Values Which Allow Design of a Three Module Transverse Flow Gas Lens with Spherical Wavefront and Circular Cross Section Output. See Eqs. (14) and (15). Note $A_1 = A_2 = A_3 = A$. Due to circular symmetry, y and z have been replaced by $r = (y^2 + z^2)^{1/2}$. A collimated input beam is assumed.

$\frac{\dot{r}_3}{Ar_o}$	$\frac{r_3}{r_o}$	AL_1	AL_2	AL_3	$A(L_1+L_2+L_3)$	$\frac{1}{AR}$
0.000	1.000	0.000	0.000	0.000	0.000	0.000
0.200	1.039	0.099	0.199	0.097	0.395	0.192
0.400	1.150	0.195	0.390	0.182	0.767	0.348
0.600	1.315	0.285	0.569	0.248	1.102	0.456
0.800	1.519	0.369	0.733	0.298	1.399	0.527
1.000	1.749	0.446	0.881	0.335	1.661	0.572
1.200	1.997	0.517	1.016	0.362	1.895	0.601
1.400	2.258	0.583	1.138	0.384	2.104	0.620
1.600	2.528	0.644	1.249	0.401	2.294	0.633
1.800	2.806	0.701	1.350	0.415	2.466	0.642
2.000	3.088	0.755	1.444	0.426	2.624	0.648
2.200	3.375	0.805	1.530	0.436	2.770	0.652
2.400	3.665	0.853	1.609	0.444	2.906	0.655
2.600	3.958	0.898	1.684	0.451	3.032	0.657
2.800	4.253	0.941	1.753	0.457	3.151	0.658
3.000	4.550	0.982	1.818	0.462	3.262	0.659
100.000	158.373	3.677	5.298	0.584	9.559	0.631

III. CONCLUDING REMARKS

The effect of a streamwise variation of the index of refraction has been neglected [e.g., Eq. (7b)]. The latter variation can be caused by wall shear-induced pressure gradient, by wall heat transfer-induced centerline temperature gradient, and by laser heating of the flowing gas. A linear streamwise index of refraction variation acts like a wedge and tends to tilt the laser beam. This effect can be compensated for by the subdivision of each module into three sections with counterflow in the central section as indicated in Fig. 8. The width of the central section

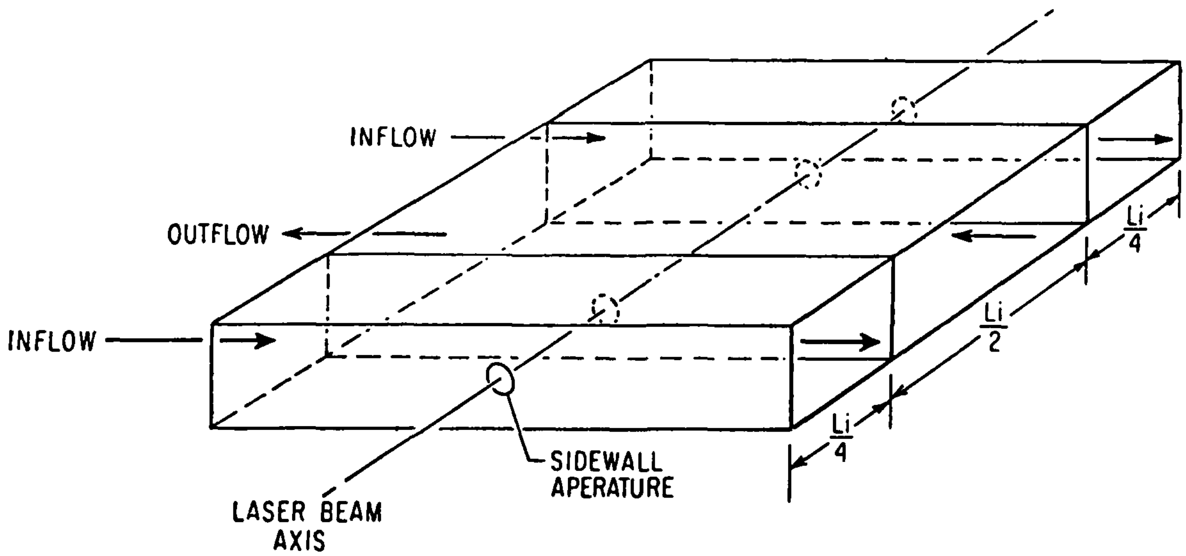

Fig. 8. A Schematic Diagram Which Indicates the Use of Counter Flow to Compensate for a Linear Streamwise Variation of Index of Refraction. A single module is shown. The central section has twice the width of the two end sections.

is twice the width of each end section. The configuration in Fig. 8 provides exact compensation for a linear streamwise variation in refractive index. It is preferable, however, to avoid significant streamwise gradients by judicious choice of flow variables. For example, an increase in flow velocity v will reduce the streamwise temperature gradient.

Each module requires at least two sidewalls (e.g., Fig. 7). Each sidewall requires an aperture to allow transit of the laser beam. The sidewalls and apertures are potential sources of beam quality degradation. This degradation can be minimized by: (a) use of thermal insulator sidewall material so as to minimize the sidewall impact on the gas flow temperature profile; (b) use of small sidewall aperture diameters; and (c) use of low values of the design parameter A so as to increase the optical path length within each module and thereby reduce the relative importance of the aperture region.

The transverse flow gas lens concept has been described in terms of cooled plates to produce beam divergence. The use of heated plates will produce a reversal in the gas flow temperature gradients and a resultant positive lens. The latter may be used for collimating a diverging beam or for focusing. When $T_w > T_o$, the parameter A_i is imaginary [Eq. (7c)] and the hyperbolic functions are replaced by trigonometric functions in Eqs. (8) to (14) as previously noted.

REFERENCES

1. D. Marcuse and S. E. Miller, "Analysis of a Tubular Gas Lens," Bell System Technical Journal, 1758-1782 (July 1964).

2. W. H. Christiansen, "Gas Optics Applicable to the Free Electron Laser," Seventh International Symposium on Gas Flow and Chemical Lasers, Vienna, 22-26 August 1988.

3. W. M. Roshenow and J. P. Hartnett, Handbook of Heat Transfer, McGraw-Hill Book Co., New York, 8-85 (1973).

4. M. Born and E. Wolf, Principles of Optics, Pergamon Press, New York, 122 (1970).

LABORATORY OPERATIONS

The Aerospace Corporation functions as an "architect-engineer" for national security projects, specializing in advanced military space systems. Providing research support, the corporation's Laboratory Operations conducts experimental and theoretical investigations that focus on the application of scientific and technical advances to such systems. Vital to the success of these investigations is the technical staff's wide-ranging expertise and its ability to stay current with new developments. This expertise is enhanced by a research program aimed at dealing with the many problems associated with rapidly evolving space systems. Contributing their capabilities to the research effort are these individual laboratories:

Aerophysics Laboratory: Launch vehicle and reentry fluid mechanics, heat transfer and flight dynamics; chemical and electric propulsion, propellant chemistry, chemical dynamics, environmental chemistry, trace detection; spacecraft structural mechanics, contamination, thermal and structural control; high temperature thermomechanics, gas kinetics and radiation; cw and pulsed chemical and excimer laser development, including chemical kinetics, spectroscopy, optical resonators, beam control, atmospheric propagation, laser effects and countermeasures.

Chemistry and Physics Laboratory: Atmospheric chemical reactions, atmospheric optics, light scattering, state-specific chemical reactions and radiative signatures of missile plumes, sensor out-of-field-of-view rejection, applied laser spectroscopy, laser chemistry, laser optoelectronics, solar cell physics, battery electrochemistry, space vacuum and radiation effects on materials, lubrication and surface phenomena, thermionic emission, photosensitive materials and detectors, atomic frequency standards, and environmental chemistry.

Electronics Research Laboratory: Microelectronics, solid-state device physics, compound semiconductors, radiation hardening; electro-optics, quantum electronics, solid-state lasers, optical propagation and communications; microwave semiconductor devices, microwave/millimeter wave measurements, diagnostics and radiometry, microwave/millimeter wave thermionic devices; atomic time and frequency standards; antennas, rf systems, electromagnetic propagation phenomena, space communication systems.

Materials Sciences Laboratory: Development of new materials: metals, alloys, ceramics, polymers and their composites, and new forms of carbon; nondestructive evaluation, component failure analysis and reliability; fracture mechanics and stress corrosion; analysis and evaluation of materials at cryogenic and elevated temperatures as well as in space and enemy-induced environments.

Space Sciences Laboratory: Magnetospheric, auroral and cosmic ray physics, wave-particle interactions, magnetospheric plasma waves; atmospheric and ionospheric physics, density and composition of the upper atmosphere, remote sensing using atmospheric radiation; solar physics, infrared astronomy, infrared signature analysis; effects of solar activity, magnetic storms and nuclear explosions on the earth's atmosphere, ionosphere and magnetosphere; effects of electromagnetic and particulate radiations on space systems; space instrumentation.